

High-power all-fiber 1.0/1.5 μm dual-band pulsed MOPA source

Xiaogang Ge (葛小钢)¹, Jun Yu (余军)¹, Weiqi Liu (刘伟琪)¹,
Shuangchen Ruan (阮双琛)¹, Chunyu Guo (郭春雨)^{1,*}, Yewang Chen (陈业旺)¹,
Peiguang Yan (闫培光)¹, and Ping Hua (华萍)^{1,2}

¹Shenzhen Key Laboratory of Laser Engineering, Key Laboratory of Advanced Optical Precision Manufacturing Technology of Guangdong Higher Education Institutes, College of Optoelectronic Engineering, Shenzhen University, Shenzhen 518060, China

²Optoelectronics Research Centre, University of Southampton, Southampton SO17 1BJ, UK

*Corresponding author: cyguo@szu.edu.cn

Received June 17, 2017; accepted September 8, 2017; posted online December 26, 2017

The simultaneous dual-band pulsed amplification is demonstrated from an Er/Yb co-doped fiber (EYDF), and consequently a high-power all-fiber single-mode 1.0/1.5 μm dual-band pulsed master oscillator power amplifier (MOPA) laser source is realized for the first time, to the best of our knowledge, based on one singlegain fiber. The simultaneous outputs at 1061 and 1548 nm of the laser source have the maximum powers of 10.7 and 25.8 W with the pulse widths of 9.5 ps and 2 ns and the pulse repetition rates of 178 and 25 MHz, respectively. This EYDF MOPA laser source is seeded by two separate preamplifier chains operating at 1.0 and 1.5 μm wavebands. The dependence of the laser output powers on the length of the large-mode area EYDF, the ratio of the powers of the two signals launched into the booster amplifier, and the wavelength of the 1 μm seed signal are also investigated experimentally.

OCIS codes: 140.3510, 140.3280, 140.3538.

doi: 10.3788/COL201816.020010.

Fiber lasers have various advantages, including excellent beam quality, high conversion efficiency, broad gain bandwidth, high thermal stability, and robust operation. A high-power pulsed fiber laser is widely welcomed in various applications, such as remote sensing, light detection, materials processing, laser radar, biomedicine, free-space communications, and fundamental science^[1,2]. In recent years, many remarkable results have been obtained with such high-power pulsed fiber lasers operating in the 1^[3-5], 1.5^[6-8], and 2 μm regions^[9,10]. However, these researches were all focused on single waveband output.

Simultaneous dual-band lasers have numerous applications in difference-, harmonic-, and sum-frequency generation, coherent anti-Stokes Raman scattering (CARS) microscopy, fiber optic sensors, and ultra-wideband super-continuum generation. In the past few years, various techniques have been used to assemble dual-band laser sources. Some researchers have built dual-band fiber laser sources by using two separate cavities with separate gain media^[11,12]. Another way to obtain simultaneous oscillation of two wavebands is based on cascaded erbium- and ytterbium-doped fibers that share the same cavity, producing two-color pulses (1040 and 1550 nm) with a total output power of 3 mW^[13]. In order to reduce complexity, an alternative approach to realize a dual-band laser source is to combine different rare-earth dopants in one fiber. In recent years, dual-band laser emissions have been demonstrated by using Er/Nd co-doped fibers^[14,15] and Er/Yb co-doped fibers (EYDFs).

In traditional EYDF lasers (EYDFLs) and EYDF amplifiers (EYDFAs), the Yb band amplified spontaneous emission (Yb-ASE) has been widely considered as a main obstacle for the power scaling and stable operation due to the resulting parasitic lasing, self-pulsing, or even system damage^[16-18]. Simultaneous oscillation^[16-19] or seeding^[20,21] of a 1 μm band continuous wave (CW) laser with the 1.5 μm band signal is an effective method for EYDFLs and EYDFAs to suppress the Yb-ASE, avoid the Yb band spurious lasing, and improve the efficiency of Er band lasing. However, the output of the amplified 1 μm laser is commonly undesirable for these systems and usually reabsorbed for a higher 1.5 μm efficiency or separated from 1.5 μm emission. On the contrary, some researchers have exploited these co-oscillating or co-seeding methods to demonstrate 1.0/1.5 μm dual-band fiber lasers. In Ref. [22], the milliwatt-level CW dual-band fiber laser oscillating at 1060 and 1550 nm has been accomplished by use of a specially composition-designed EYDF. And then in Ref. [23], an all-fiber setup with multiwatt-level CW outputs at 1064 and 1548 nm was reported based on the co-seeding for an EYDFA. In Ref. [24], a 1.0/1.5 μm dual-band linearly polarized all-fiber laser with a 0.65 W CW output power at each wavelength was reported by means of co-oscillating with two pairs of fiber Bragg gratings (FBGs). Apart from the above dual-band CW results from EYDFs, Yang *et al.* reported a dual-seeded EYDFA with 6.4 W 1550 nm pulsed and 13 W 1064 nm CW laser outputs^[25]. Although many CW dual-band lasers reported to-date, as far as we know, neither the feasibility of

simultaneous dual-band pulsed amplification from an EYDF nor the the corresponding high-power 1.0/1.5 μm dual-band pulsed fiber laser have been demonstrated up to now.

In this Letter, we report for the first time, to the best of our knowledge, the simultaneous amplification of dual-band pulses from an EYDF and a corresponding high-power all-fiber single-mode dual-band pulsed fiber laser with simultaneous outputs of 10.7 W at 1061 nm and 25.8 W at 1548 nm. This laser source was based on a master oscillator power amplifier (MOPA) structure seeded by two separate fiber preamplifier chains operating at 1 and 1.5 μm , respectively. To optimize the performance of this dual-band laser source with comparable output powers, the influence of the length of the large-mode area (LMA) EYDF, the ratio between the two seed powers and the wavelength of the 1 μm seed signal were experimentally investigated.

The high-power single-mode dual-band pulsed fiber laser is schematically shown in Fig. 1. It is based on a MOPA structure seeded by a 1 μm wavelength-tunable fiber preamplifier and 1.5 μm fiber preamplifier chains, which were simultaneously amplified in the LMA-EYDFA (dual-band booster amplifier).

The seed signal at 1.0 μm was provided by a passively mode-locked fiber laser based on the nonlinear polarization rotation (NPR) technique with 8.5 ps output pulses at the pulse repetition rate (PRR) of 22 MHz, and it was then preamplified through cascaded Yb-doped fiber amplifiers (YDFAs) similar to the setup in Ref. [26]. The cascaded amplifiers consisted of three YDFAs core-pumped by three 480 mW single-mode 976 nm laser diodes (LDs). In addition, a repetition rate increasing system was adopted after the second YDFA to octuple the repetition rate and reduce the peak power of the pulses, so as to suppress the nonlinear effects. This was followed by a double-clad (DC) YDFA with a 3.1-m-long Yb-doped fiber (YDF) cladding pumped by a 20 W fiber pigtailed 976 nm multimode LD through a $(2 + 1) \times 1$ fiber combiner. The DC-YDF has a core/cladding diameter of 15/130 μm and an effective core/cladding numerical aperture (NA) of 0.08/0.46 with the cladding absorption of 5.4 dB/m at 976 nm. Each stage was separated by an

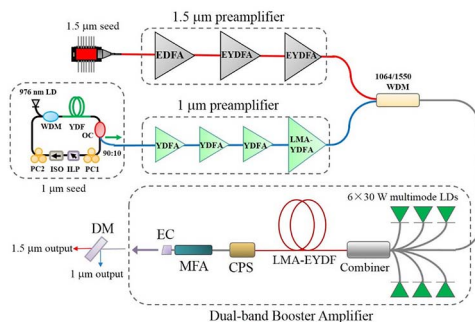


Fig. 1. Experimental setup of the high-power single-mode 1.0/1.5 μm dual-band pulsed fiber laser.

isolator (ISO) that ensured unidirectional operation. This four-stage preamplifier chain delivered an average power of up to 2 W at the PRR of 178 MHz. By carefully adjusting the polarization controllers (PCs) inside the mode-locked fiber ring laser, output pulses at different wavelengths were realized.

The other seed signal at 1.5 μm was provided by a fiber-pigtailed 1548 nm pulsed LD with 2 ns output pulses at the PRR adjustable from 1 to 150 MHz, and it was pre-amplified through one stage of an Er-doped fiber amplifier (EDFA) and two stages of EYDFAs before launching into the LMA-EYDFA. The EDFA was based on a 19-m-long Er-doped fiber (EDF) pumped by a 550 mW single-mode 976 nm LD. The two EYDFAs are comprised of 4.9 and 3.9 m DC-EYDFs with a 6/125 core/cladding diameter and were pumped by two 20 W multimode LDs through two $(2 + 1) \times 1$ fiber combiners. ISOs were used between each stage to prevent feedback from the latter stage. Through the use of three-stage preamplifier chain, the average output power of the 1548 nm seed could be amplified to 2 W to feed into the LMA-EYDFA.

The two signals were injected into the booster amplifier (LMA-EYDFA) via a 1064/1550 nm wavelength division multiplexer (WDM). The LMA-EYDFA consisted of a short section of LMA-EYDF with a core/cladding diameter of 25/300 μm and a core/cladding NA of 0.09/0.46 with the cladding absorption of ~ 15 dB/m at 976 nm. The active fiber was forward pumped by six 30 W multimode 976 nm LDs, using a $(6 + 1) \times 1$ high-power pump combiner. A cladding power stripper (CPS) was introduced at the other end of the LMA-EYDF to strip off the unabsorbed pump light. A mode field adapter (MFA) with a 25/300 μm LMA fiber (0.09/0.46 NA) at the input port and a 6/125 μm HI1060 fiber at the output port was incorporated after the CPS to strip off the high-order modes, consequently achieving single-mode output. The measured losses for the fundamental mode are 0.39 and 0.35 dB, respectively, at 1.0 and 1.5 μm . Finally, an angled end cap (EC) was arranged at the output port of the system to avoid back reflection and end facet damage. A dichroic mirror (DM), which has a high reflection at 900–1200 nm and a high transmission at 1200–1600 nm, was used to separate the 1 and 1.5 μm output beams.

In our experiment, the output spectra were measured by an optical spectrum analyzer (OSA, YOKOGAWA AQ6370B). The output power was monitored by an optical power meter (OPM) and the pulse trains were measured by a 1 GHz digital oscilloscope (Tektronix DPO 7104C) together with a 45 GHz InGaAs photodetector (New Focus 1014).

In order to achieve comparable power levels for the dual-band outputs, three different lengths (95, 80, and 65 cm) of the LMA-EYDFs were investigated. The wavelengths of 1 and 1.5 μm signals were 1053 and 1548 nm, respectively, while the average powers of the two signals launched into the LMA-EYDFA were 1 and 0.7 W, respectively. The output powers at 1 and 1.5 μm versus pump power are shown in Fig. 2. At 150 W incident pump power,

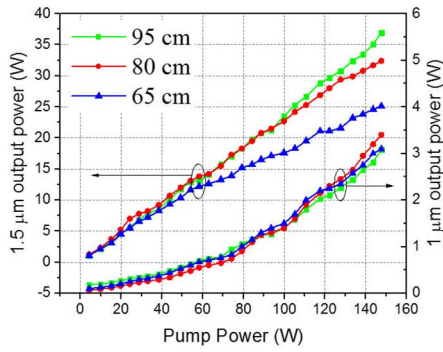


Fig. 2. (Color online) Output powers of the two wavelengths versus pump power for three different lengths of LMA-EYDFs.

the output powers of 1/1.5 μm were 3.08/36.9, 3.4/32.4, and 3.1/25.1 W for the fiber lengths of 95, 80, and 65 cm, respectively. This indicates that the longer length of LMA-EYDF increases the reabsorption of the 1 μm emission and, thus, limits its output power, while the shorter length is unable to provide sufficient gain for the amplification of the 1 μm laser^[27]. Therefore, an 80 cm LMA-EYDF was preferred in our dual-band amplification experiment.

Secondly, to study the effects of the ratio between 1 and 1.5 μm seed powers launched into the LMA-EYDFA, three different input power pairs (1 W:0.7 W, 1 W:1 W, and 1 W:1.3 W) were examined. Figure 3 plots the output powers of the two wavelengths versus pump power. It can be seen that the 1 μm output power is affected by the 1.5 μm input power due to gain competition. In the EYDF, the gain competition between 1 and 1.5 μm emission is caused by the cross-relaxation energy transfer from Yb ions to Er ions. Unlike the gain competition in a single active-ion-doped fiber, which sometimes disturbs the stability of dual-wavelength operation^[28], the gain competition in EYDF does not influence the stability of dual-band outputs, and stable dual-band operation exists both in the CW regime^[24,25] and the pulsed regime^[29]. When the 1.5 μm input power varied from 1.3 to 0.7 W, the 1 μm output power increases from 3.1 to 4.4 W. This can be explained by the fact that the decrease of 1.5 μm seed signal reduces the depopulation rate of the Er-ions,

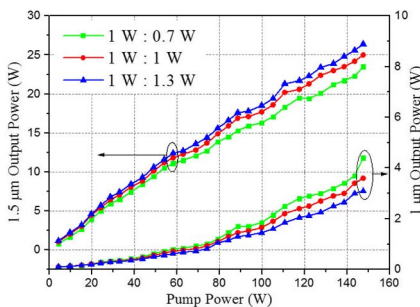


Fig. 3. (Color online) Output powers of the two wavelengths versus pump power for three different power ratios between the 1 and 1.5 μm signals.

and, therefore, the energy transfer rate from Yb to Er ions increases the Yb-ion population in the upper energy state, thus promoting the 1 μm amplification. In contrast, sufficient input of the 1.5 μm seed signal is beneficial for the 1.5 μm amplification and for suppressing the emission at the Yb band.

Thirdly, in order to investigate the influence of the 1 μm seed wavelength on the performance of the dual-band outputs, five operating wavelengths (1039, 1046, 1053, 1061, and 1071 nm) at the 1 μm band were examined. Figure 4(a) shows the output spectra at 1 μm , while the inset represents the autocorrelation trace of the 1 μm seed. The seed powers of 1 and 1.5 μm launched into the LMA-EYDFA were 1 and 0.7 W, respectively. Plots showing the 1 and 1.5 μm output powers versus pump power are depicted in Fig. 4(b). It can be seen that the output power is strongly dependent on the wavelength of the 1 μm seed signal. For the case of 150 W pump power, the output powers at 1/1.5 μm were 1.8/25.1, 3.1/24.7, 4/22.7, 5.1/21.9, and 4.2/23 W for the 1 μm seed wavelength of 1039, 1046, 1053, 1061, and 1071 nm, respectively. The 1 μm output power increased significantly as the wavelength of the 1 μm seed signal was adjusted from 1039 to 1061 nm, and then slightly dropped off when it reached 1071 nm. It is clear from Fig. 4(a) that the 1061 nm wavelength lies at the peak of the available gain bandwidth, so it experiences the highest gain, while other wavelengths lying away from the gain peak see lower overall gain and, thus, lower output power^[30].

Therefore, the 1061 nm wavelength was chosen for dual-band amplification in our experiment. In order to further increase the 1 μm output power and to achieve comparable

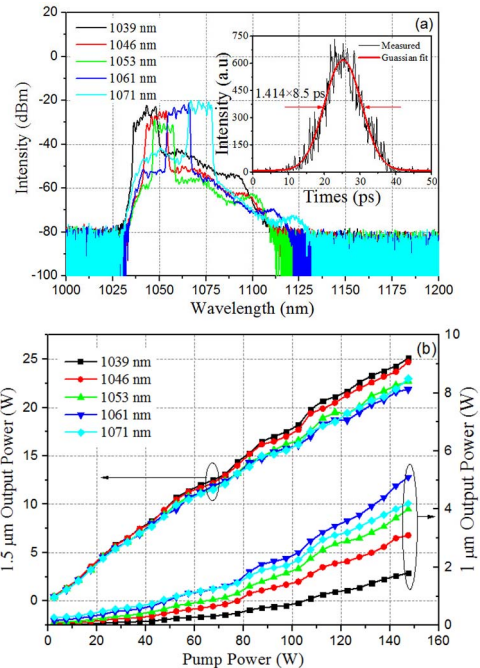


Fig. 4. (Color online) (a) Output spectra at 1 μm (OSA resolution is 0.5 nm). Inset shows the autocorrelation trace of the 1 μm seed. (b) The 1 and 1.5 μm output powers versus pump power.

power levels of the two wavebands, the 1061 nm seed power launched into the LMA-EYDFA was increased to 1.66 W, while the 1548 nm seed power was decreased to 0.5 W. The output powers of the 1 and 1.5 μm signals versus pump power are plotted in Fig. 5(a). The slope efficiency of the 1.0 μm signal rose significantly from 3.1% up to 8.2% with the pump power higher than 80 W, whereas the slope efficiency of the 1.5 μm signal dropped from 16.9% down to 12.1%. However, the slope efficiency of the outputs from the CPS and the MFA stayed almost constant, about 33.6% and 20.3%, as the pump power increased, as can be seen from Fig. 5(b). This is caused by the bottle-necked energy transfer between the Yb and Er ions at the high pump power level^[20]. The high pump rate

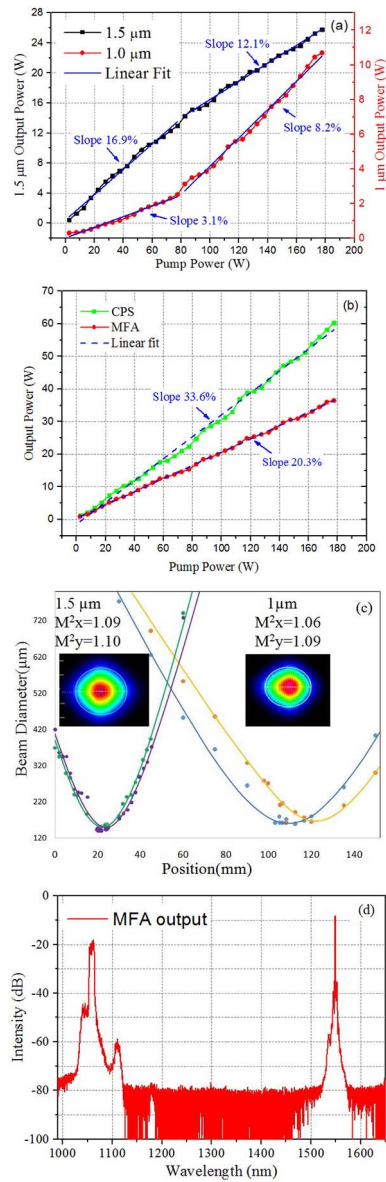


Fig. 5. (Color online) (a) The 1 and 1.5 μm output powers versus pump power. (b) Output powers from the CPS and the MFA versus pump power. (c) Beam quality of 1 and 1.5 μm emission. (d) Emission spectra of the dual-band pulsed fiber laser at the maximum pump power (OSA resolution is 0.5 nm).

corresponds to a dramatically increased inversion population of the Yb ions, and, consequently, the Yb-band gain grows rapidly. Thus, the slope efficiency of the 1.0 μm signal rises obviously, and the slope efficiency of the 1.5 μm signal drops at the same time. It is observed that when the pump power of the LMA-EYDFA was 177.5 W, the total output powers from the CPS and the MFA were 60.3 and 36.5 W, respectively, and the maximum output powers at the 1.0 and 1.5 μm wavebands were 10.7 and 25.8 W, respectively. The beam quality of the 1 and 1.5 μm emissions after the DM have been measured with M^2 factors of 1.08 and 1.10, as shown in Fig. 5, which demonstrates the single operation of this dual-band fiber source. The high loss between the CPS output and the MFA output results mainly from the high-order modes generated in the LMA-EYDF.

The output spectrum from the MFA at the maximum output power is shown in Fig. 5(c). No significant spectral broadening in the 1.5 μm range was observed, while the signature of stimulated Raman scattering (SRS) was observed at 1120 nm in the 1 μm range. However, the laser peak at 1061 nm remained 40 dB above the SRS peak at the maximum power level, which indicates that most of the output power concentrated in the signal wavelength. Output pulse trains at 1 and 1.5 μm at the maximum output power are shown in Fig. 6. The pulse width of the amplified 1 μm signal was measured to be 9.5 ps, while the pulse width of the amplified 1.5 μm signal remained 2 ns.

In conclusion, we demonstrate a dual-band high-power single-mode pulsed MOPA laser source operating at 1.0 and 1.5 μm through a simultaneous dual-band pulsed amplification based on one single EYDF gain fiber. Through the optimization of three conditions (the length of the LMA-EYDF, the ratio of the two input seed powers, and the wavelength of the 1 μm signal), this laser source produces simultaneous single-mode outputs of 10.7 W at 1061 nm with 9.5 ps pulses at the PRR of 178 MHz and 25.8 W at 1548 nm with 2 ns pulses at the PRR of 25 MHz. This laser source is a promising candidate for efficient ultra-wideband supercontinuum generation. It is to be noted here that this research is focused on the simultaneous generation of dual-band pulses in a single gain fiber. In our future work, we will investigate the synchronized dual-band EYDFL^[29] mode-locked by some broadband saturable absorbers^[31–35] and use this as the dual-band seed laser for amplification to realize the high-power dual-band synchronized pulsed fiber laser source suitable for different-frequency mid-IR generation.

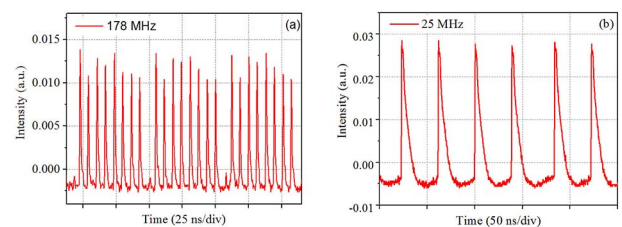


Fig. 6. Output pulse trains at (a) 1 μm and (b) 1.5 μm at the maximum output power.

This work was supported by the National Natural Science Foundation of China (NSFC) (No. 61308049), the National High-tech R&D Program of China (863 Program) (No. 2015AA021102), the Outstanding Young Teacher Cultivation Projects in Guangdong Province (No. YQ2015142), the Shenzhen Science and Technology Project (Nos. JCYJ20160520161351540 and JCYJ20160427105041864).

References

1. J. Limpert, F. Roser, T. Schreiber, and A. Tunnermann, *IEEE J. Sel. Top. Quantum Electron.* **12**, 233 (2006).
2. D. Richardson, J. Nilsson, and W. Clarkson, *J. Opt. Soc. Am. B* **27**, B63 (2010).
3. S. P. Chen, H. W. Chen, J. Hou, and Z. J. Liu, *Opt. Express* **17**, 24008 (2009).
4. H. W. Chen, Y. Lei, S. P. Chen, J. Hou, and Q. S. Lu, *Appl. Phys.* **B109**, 233 (2012).
5. R. Song, J. Hou, S. Chen, W. Yang, and Q. Lu, *Appl. Opt.* **51**, 2497 (2012).
6. C. Yang, S. Xu, S. Mo, C. Li, Z. Feng, D. Chen, Z. Yang, and Z. Jiang, *Opt. Express* **21**, 12546 (2013).
7. I. Pavlov, E. Dulgergil, E. Ilbey, and F. O. Ilday, *Opt. Lett.* **39**, 2695 (2014).
8. K. Guo, X. Wang, P. Zhou, and B. Shu, *Appl. Opt.* **54**, 504 (2015).
9. Y. Tang, X. Li, Z. Yan, X. Yu, Y. Zhang, and Q. J. Wang, *IEEE J. Sel. Top. Quantum Electron.* **20**, 537 (2014).
10. D. Ouyang, J. Zhao, Z. Zheng, S. Ruan, C. Guo, P. Yan, and W. Xie, *IEEE Photon. J.* **7**, 1 (2015).
11. D. G. Lancaster, D. Richter, R. F. Curl, F. K. Tittel, L. Goldberg, and J. Kopolow, *Opt. Lett.* **24**, 1744 (1999).
12. C. Erny, K. Moutzouris, J. Biegert, D. Kühlke, F. Adler, A. Leitenstorfer, and U. Keller, *Opt. Lett.* **32**, 1138 (2007).
13. M. Rusu, R. Herda, and O. G. Okhotnikov, *Opt. Lett.* **29**, 2246 (2004).
14. Y. Kimura and M. Nakazawa, *Appl. Phys. Lett.* **53**, 1251 (1988).
15. J. M. Battiato, T. Morse, and R. K. Kostuk, *IEEE Photon. Technol. Lett.* **9**, 913 (1997).
16. J. K. Sahu, Y. Jeong, D. J. Richardson, and J. Nilsson, *Opt. Commun.* **227**, 159 (2003).
17. J. Yoonchan, Y. Seongwoo, C. A. Coderaard, J. Nilsson, J. K. Sahu, D. N. Payne, R. Horley, P. W. Turner, L. Hickey, A. Harker, M. Lovelady, and A. Piper, *IEEE J. Sel. Top. Quantum Electron.* **13**, 573 (2007).
18. Q. Han, Y. Yao, Y. Chen, F. Liu, T. Liu, and H. Xiao, *Opt. Lett.* **40**, 2634 (2015).
19. G. Sobon, P. Kaczmarek, A. Antonczak, J. Sotor, and K. M. Abramski, *Opt. Express* **19**, 19104 (2011).
20. V. Kuhn, P. Weßels, J. Neumann, and D. Kracht, *Opt. Express* **17**, 18304 (2003).
21. Q. Han, Y. He, Z. Sheng, W. Zhang, J. Ning, and H. Xiao, *Opt. Lett.* **36**, 1599 (2011).
22. J. Bouillet, L. Lavoute, B. A. Desfarges, V. Kermène, and P. Roy, *Opt. Express* **14**, 3936 (2006).
23. K. Krzempek, G. Sobon, and K. M. Abramski, *Opt. Express* **21**, 20023 (2013).
24. A. R. El-Damak, J. Chang, J. Sun, C. Xu, and X. Gu, *IEEE Photon. J.* **5**, 1501406 (2013).
25. W. Yang, K. Yin, B. Zhang, G. Xue, and J. Hou, *Appl. Phys.* **B116**, 169 (2014).
26. L. Huaiqin, G. Chunyu, R. Shuangchen, W. Ruhua, Y. Jun, and L. Weiqi, *IEEE Photon. J.* **6**, 1 (2014).
27. Q. Han, J. Ning, and Z. Sheng, *IEEE J. Quantum Electron.* **46**, 1535 (2010).
28. Y. Cui and X. Liu, *Opt. Express* **21**, 18969 (2013).
29. C. Guo, W. Liu, S. Ruan, J. Yu, Y. Chen, P. Yan, J. Wang, S. Jain, and P. Hua, *IEEE Photon. J.* **9**, 1 (2017).
30. D. Sliwinska, P. Kaczmarek, G. Sobon, and K. M. Abramski, *J. Lightwave Technol.* **31**, 3381 (2013).
31. H. Zhang, S. B. Lu, J. Zheng, J. Du, S. C. Wen, D. Y. Tang, and K. P. Loh, *Opt. Express* **22**, 7249 (2014).
32. S. Chen, C. Zhao, Y. Li, H. Huang, S. Lu, H. Zhang, and S. Wen, *Opt. Mater. Express* **4**, 587 (2014).
33. P. Yan, R. Lin, H. Chen, H. Zhang, A. Liu, H. Yang, and S. Ruan, *IEEE Photon. Technol. Lett.* **27**, 264 (2015).
34. X. Liu, Y. Cui, D. Han, X. Yao, and Z. Sun, *Sci. Rep.* **5**, 9101 (2015).
35. Y. Cui, F. Lu, and X. Liu, *Sci. Rep.* **6**, 30524 (2016).